

Oxy-steam combustion: the effect of coal rank and steam concentration on combustion characteristics

Ana I. Escudero, María Aznar, Luis I. Díez*

Department of Mechanical Engineering, Joint Institute University of Zaragoza-CIRCE,
University of Zaragoza, María de Luna s/n, 50018 Zaragoza, Spain

Abstract

This paper addresses the experimental investigation of coal combustion characteristics (ignition, burnout and NO formation) under oxy-steam combustion conditions. Two coals are selected in order to compare the effect of the rank: bituminous and sub-bituminous ones. The experiments have been conducted in an electrically-heated entrained flow reactor for a set of O₂/N₂, O₂/CO₂ and O₂/H₂O/CO₂ atmospheres, with O₂ concentrations up to 35% and H₂O concentrations up to 40%. Regarding ignition, 10% H₂O reduces ignition temperature (max. 16–19 K) but the trend is reversed when supplying additional steam to 25% and 40%. This behaviour is similar for both coals, with slight larger variations in the case of the low rank coal. Burnout degree of the sub-bituminous coal is barely affected by the steam concentration since all observed conversions are very high. Larger increments (up to 6.1 percentage points) are obtained for the bituminous coal, with a maximum burnout degree for the 25/35% H₂O/O₂ atmosphere. A very different effect of steam on NO formation is found depending on the coal rank. Significant reduction rates are observed for the bituminous coal in comparison to the dry O₂/CO₂ atmospheres, with a maximum diminution of 24% when 40% H₂O replaces CO₂. On the contrary, the higher volatile content in the sub-bituminous coal leads to NO increments up to 9%. For all the combustion characteristics studied, the increase of O₂ concentrations attenuates the effects caused by the steam addition.

Keywords

Oxy-combustion; Steam moderation; Coal rank; Ignition; Burnout; NO formation

* Corresponding autor. Tel.: +34 976 762 564. E-mail: luisig@unizar.es

29 1. Introduction.

30 A large deployment of renewable energies is currently being required to obtain a
31 significant reduction of CO₂ emissions, as an urgent target to mitigate the effects of
32 global warming. Nevertheless, coal still contributed in 2018 to the 38.5% of the world
33 electricity production [1]. This global frame turns CO₂ capture technologies as essential
34 to match the pathways of the Paris Agreement.

35 Oxy-fuel combustion is one of the capture technologies suitable for coal-fired power
36 plants. Many results have been obtained in the last years concerning oxy-coal
37 combustion, including lab-, pilot- and demo-scale facilities. A related concept, but
38 significantly new and different, is the so-called oxy-steam combustion. It consists on the
39 full avoidance of the flue gases recycle, replacing CO₂ by H₂O to dilute the oxygen.
40 Condensed water from the flue gases is re-boiled and redirected to the furnace, acting as
41 O₂ dilution [2, 3]. The main advantages of this alternative are simplified plant operation,
42 reduction of auxiliary consumptions and lower air in-leakages. Replacement of CO₂ by
43 H₂O in the firing atmosphere may bring several differences in the combustion
44 characteristics of solid fuels, due to their different thermophysical and chemical
45 behaviour. Some coupled phenomena like volatiles oxidation, char reactivity and
46 conversion, gas-particle heat transfer and pollutants formation/depletion, have to be well
47 characterized to determine the consequences of shifting from the O₂/CO₂ atmosphere to
48 the O₂/H₂O one.

49 Few studies are available so far addressing oxy-steam combustion of pulverized coal,
50 most of them focused on the ignition behaviour of single/few particles, under different
51 steam concentrations. A summary of experiences, conditions and findings is shown in
52 Table 1. There is not a common outcome from these works, since the effect of steam on
53 ignition depends on several factors like the coal rank, the coal supply conditions (particle
54 size and flow rates), the O₂ concentration and the H₂O concentration [4].

55 Besides ignition and conversion, steam can also play a role in NO_x formation/depletion
56 mechanisms. Many studies are available, for a wide range of scales, assessing NO_x
57 behaviour for O₂/CO₂ atmospheres [11–14]. However, the effect of the steam on NO_x
58 under oxy-combustion conditions has been scarcely investigated, and with limited steam
59 rates. Moron and Rybak [15] investigated NO_x formation for hard and brown coals in an
60 oxy-fired EFR, with steam addition up to 10%. Steam lowered the NO_x levels detected.
61 Small influences were reported by Álvarez et al. [16], who conducted oxy-combustion

62 experiments for a high-volatile bituminous coal with steam concentrations in the range
 63 5–20%. Yupeng et al. [17] studied the char-nitrogen conversion for a bituminous coal,
 64 under 20% H₂O content. They found that steam addition promoted nitrogen release at
 65 low oxygen concentration, but it was inhibited at higher oxygen concentrations. To our
 66 knowledge, only the work by Zhijun et al. [18] surpassed 20% H₂O, conducting tests up
 67 to 40% H₂O for anthracite and bituminous coals in an oxy-fired DTF. These authors
 68 reported steam rates minimizing NO emissions, with a competitive effect between CO₂
 69 and H₂O concentrations in the atmosphere.

70

Reference	Coal type	Facility	Atmosphere	% H ₂ O	Main outcomes
Kops et al., 2019 [5]	Sub-bituminous	DTF + high speed camera	O ₂ /N ₂ /H ₂ O O ₂ /CO ₂ /H ₂ O	0–10%	Shortening of ignition delay time due to steam addition
Riaza et al., 2011 [6]	Anthracite Bituminous	EFR	O ₂ /N ₂ /H ₂ O O ₂ /CO ₂ /H ₂ O	0–20%	Increase of ignition temperature when replacing CO ₂ by H ₂ O
Pratono and Zhang, 2016 [4]	Bituminous Sub-bituminous	EFR + high speed camera	O ₂ /N ₂ /H ₂ O O ₂ /CO ₂ /H ₂ O	0–26%	The lower the rank of the coal, the higher the effect of the steam Negligible steam effect for O ₂ enriched atmospheres
Cai et al., 2016 [7]	Bituminous	DTF + high speed camera	O ₂ /CO ₂ /H ₂ O	0–30%	Negligible effect for steam up to 20% Significant ignition overtake for 30%
Escudero et al., 2020 [8]	Anthracite	EFR	O ₂ /CO ₂ /H ₂ O	0–40%	Decrease of ignition temperature for low steam rates, increase for the higher ones
Zou et al., 2015 [9]	Bituminous	DTF + high speed camera	O ₂ /H ₂ O	50–79%	Shortening of ignition delay time due to steam addition
Hao et al., 2019 [10]	Bituminous	SPR + high speed camera	O ₂ /H ₂ O	50–79%	Shortening of ignition delay time due to steam addition

71

72 **Table 1.-** Summary of experimental works related to oxy-coal ignition under steam-containing atmospheres.
 73 DTF = drop tube furnace. EFR = entrained flow reactor. SPR = single particle reactor.
 74

75

76 Our study aims to widen the limited knowledge about coal oxy-combustion with large
 77 steam additions as CO₂ replacement. In particular, scarce results are reported for
 78 low-rank coals. This paper presents a detailed, comprehensive characterization of the
 79 oxy-steam combustion characteristics (ignition, burnout and NO_x formation) for a pair of
 80 coals: one sub-bituminous and one bituminous, also seeking the effect of the coal rank on

81 the results. The experiments are not focused on single/few particles, but on a steady
 82 flowrate in an entrained flow reactor, operated under atmospheres containing up to 40%
 83 H₂O and up to 35% O₂.

84 2. Experiments.

85 2.1. Coals.

86 Two different coals were tested to comparatively study their oxy-steam combustion
 87 characteristics: 1) South-African hard coal (SA onwards), 2) blend of imported hard coals
 88 and domestic Spanish lignite, as fired in Teruel power station (CB onwards). According
 89 to ASTM D388-97 standard, the former is a medium-volatile bituminous coal and the
 90 latter and a B-type sub-bituminous one. The proximate analysis, ultimate analysis and
 91 low heating value (LHV) of these coals are listed in Table 2. Prior to tests, each sample
 92 was grounded and sieved to the size range of 75–150 μm.

93

Coal	SA	CB
ASTM D388-97	Medium-volatile bituminous	B-type sub-bituminous
Proximate analysis (% wt.)		
Moisture (as fired)	3.6	7.7
Ash (as fired)	13.1	23.4
Volatile matter (dry ash free)	30.9	46.4
Fixed carbon (dry ash free)	69.1	53.6
Ultimate analysis (% wt., dry ash free)		
Carbon	82.2	65.9
Hydrogen	4.2	3.8
Nitrogen	2.0	0.9
Sulphur	0.5	10.0
Heating value		
LHV (kJ/kg, as fired)	25 866	16 680

94

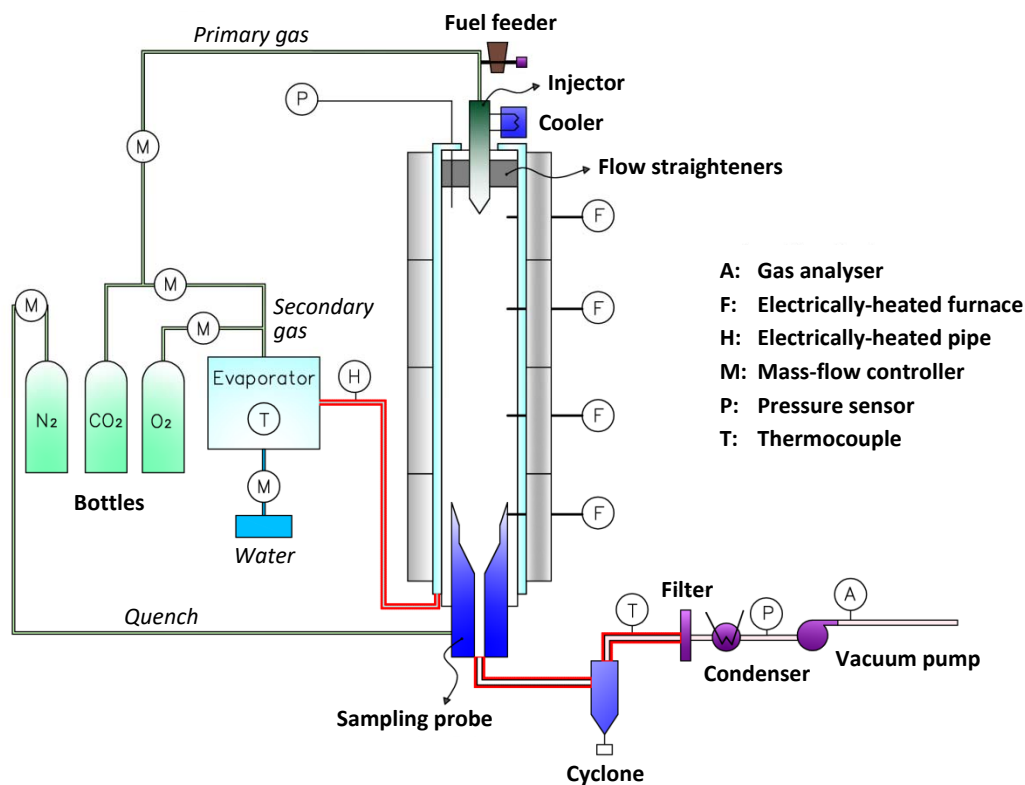
Table 2.- Coal analysis and heating value.

95 The moisture, volatile and ash contents of the coal samples were determined
 96 according to the standards ISO 5068-2:2007, ISO 562:2010 and ISO 1171:2010,
 97 respectively. The elemental analyses were performed using an elemental analyzer

98 Thermo Flash 1112. The lower heating values of the samples were determined according
99 to the standard ISO 1928:2009. These results were provided by a certified laboratory,
100 belonging to the Instituto de Carboquímica (Spanish National Research Council).

101 2.2. Experimental facility.

102 The tests were carried out in a lab-scale entrained flow reactor (EFR), with
103 continuous fuel and gas feeding systems. Figure 1 displays a diagram of the plant. The
104 reactor is made of a Kanthal alloy, with an inner diameter of 38 mm. The height can be
105 varied by a bottom-movable sampling probe, in the range 0.8–1.6 m. The reactor is
106 electrically heated by means of four independent furnaces. Maximum set-point
107 temperature for the furnaces is 1150 °C. The pulverized fuel is supplied by a mechanical
108 screw, driven by a variable-frequency motor. Several mass flow controllers provide the
109 gases from bottles, while a Coriolis flow meter is used to control water flowrate.



110

111

Figure 1.- Diagram of the lab-scale entrained flow reactor.

112 Downstream the reactor, a cyclone and a filter retains the fly solids from the gas
113 stream, and then a condenser is placed to remove most of the moisture in the flue gases.

114 Finally, a continuous emission monitoring system provides the flue gas composition at
 115 the cold-end section: non-dispersive infrared sensors for CO₂, CO SO₂, NO, and
 116 paramagnetic sensor for O₂. A more detailed description of the facility can be found
 117 elsewhere [8]. Table 3 summarizes the accuracy of the instruments used for
 118 measurements during the tests.

119

Measurement	Accuracy
Feeding gases flow rate (O ₂ , CO ₂ , N ₂)	± 0.5%
Feeding water flow rate	± 0.2%
Temperature	± 2° C
Pressure	± 3 mbar
Flue gases composition (CO ₂ , SO ₂ , CO, NO)	± 1%
Flue gases composition (O ₂)	± 1.5%

120

Table 3.- Accuracy of the on-line measurements.

121

122 2.3. Experimental procedure.

123 2.3.1. *Ignition tests.*

124 The effect of oxygen concentration (21 and 35% O₂) and steam addition (0, 10, 25 and
 125 40%) over the ignition temperature has been experimentally assessed for the two
 126 selected coals (SA bituminous and CB sub-bituminous). Thus, sixteen oxy-fired trials
 127 were conducted in the entrained flow reactor (eight for each coal). Besides, two
 128 additional tests were run under conventional combustion (21/79% O₂/N₂). The reactor
 129 was heated from room temperature to 1000 °C, at a fixed heating rate of 15 °C/min. O₂
 130 and CO₂ concentrations in flue gases were recorded to determine the ignition point. In
 131 this way, three zones are identified: 1) pre-ignition, where changes in CO₂ and O₂
 132 concentrations can be neglected, 2) ignition and conversion of particles, where CO₂
 133 concentration begins to quickly grow at the same time that O₂ concentration decreases,
 134 and 3) steady-evolution when burnout is reached, and concentrations remain constant.
 135 This indirect method has been previously used by other researchers [19, 20]. In our case,
 136 ignition temperature T_{ig} is obtained from the following approach:

137

$$\left| \frac{[X(T_{ig})] - [X(T_p)]}{[X(T_{bo})] - [X(T_p)]} \right| = 0.1 \quad (1)$$

138 where $[X(T_p)]$ is the O₂ or CO₂ molar concentration during the pre-ignition temperatures
 139 range, $[X(T_{bo})]$ is the molar concentration when steady burnout degree is reached and
 140 $[X(T_{ig})]$ is the molar concentration at the ignition temperature point. The ignition
 141 temperature was obtained by averaging the results obtained from O₂ and CO₂
 142 measurements.

143 2.3.2. Oxy-steam combustion tests.

144 Combustion experiments were carried out under different atmospheres: 21/79% O₂/N₂,
 145 21/79% O₂/CO₂, 30/70% O₂/CO₂ and 35/65% O₂/CO₂. To assess the effect of steam
 146 moderation, it was added to the oxy-firing atmospheres replacing CO₂ at the following
 147 percentages: 10%, 25% and 40% for a fixed value of oxygen excess ($\lambda = 1.25$). Thus,
 148 13 tests were carried out for each coal. In order to compare the results obtained under
 149 the different situations (coal type, % O₂, % H₂O), the experimental conditions were
 150 defined to keep the same mean residence time (3 s) for all the tests. The corresponding
 151 flow rates are presented in Tables 4 and 5. The initial reactor temperature was kept at
 152 1000 °C throughout the experimental campaign, while the reaction height was set to
 153 1.5 m. The independent effect of oxygen excess ($\lambda = 1.35$, $\lambda = 1.45$) was also analysed by
 154 means of some additional tests for the dry atmospheres.

155

Test #	Atmosphere (% vol.)	Coal flow rate (g/min)	O ₂ flow rate (g/min)	CO ₂ flow rate (g/min)	Water flow rate (g/min)
1	21/79 O ₂ /N ₂	0.55	1.39	4.59 (N ₂)	0
2	21/79 O ₂ /CO ₂	0.55	1.39	7.21	0
3	21/69/10 O ₂ /CO ₂ /H ₂ O	0.55	1.39	6.30	0.37
4	21/54/25 O ₂ /CO ₂ /H ₂ O	0.55	1.39	4.93	0.93
5	21/39/40 O ₂ /CO ₂ /H ₂ O	0.55	1.39	3.56	1.49
6	30/70 O ₂ /CO ₂	0.78	1.96	6.29	0
7	30/60/10 O ₂ /CO ₂ /H ₂ O	0.78	1.96	5.39	0.37
8	30/45/25 O ₂ /CO ₂ /H ₂ O	0.78	1.96	4.05	0.92
9	30/30/40 O ₂ /CO ₂ /H ₂ O	0.78	1.96	2.70	1.47
10	35/65 O ₂ /CO ₂	0.90	2.27	5.79	0
11	35/55/10 O ₂ /CO ₂ /H ₂ O	0.90	2.27	4.90	0.36
12	35/40/25 O ₂ /CO ₂ /H ₂ O	0.90	2.27	3.57	0.91
13	35/25/40 O ₂ /CO ₂ /H ₂ O	0.90	2.27	2.23	1.46

156 **Table 4.-** Mass flow rates during the combustion tests of the SA bituminous coal ($\lambda = 1.25$).

157

Test #	Atmosphere (% vol.)	Coal flow rate (g/min)	O ₂ flow rate (g/min)	CO ₂ flow rate (g/min)	Water flow rate (g/min)
1	21/79 O ₂ /N ₂	0.81	1.36	4.49 (N ₂)	0
2	21/79 O ₂ /CO ₂	0.81	1.36	7.06	0
3	21/69/10 O ₂ /CO ₂ /H ₂ O	0.81	1.36	6.17	0.37
4	21/54/25 O ₂ /CO ₂ /H ₂ O	0.81	1.36	4.83	0.91
5	21/39/40 O ₂ /CO ₂ /H ₂ O	0.81	1.36	3.49	1.46
6	30/70 O ₂ /CO ₂	1.12	1.90	6.11	0
7	30/60/10 O ₂ /CO ₂ /H ₂ O	1.12	1.90	5.24	0.36
8	30/45/25 O ₂ /CO ₂ /H ₂ O	1.12	1.90	3.92	0.89
9	30/30/40 O ₂ /CO ₂ /H ₂ O	1.12	1.90	2.62	1.43
10	35/65 O ₂ /CO ₂	1.30	2.19	5.60	0
11	35/55/10 O ₂ /CO ₂ /H ₂ O	1.30	2.19	4.74	0.35
12	35/40/25 O ₂ /CO ₂ /H ₂ O	1.30	2.19	3.45	0.88
13	35/25/40 O ₂ /CO ₂ /H ₂ O	1.30	2.19	2.15	1.41

158 **Table 5.-** Mass flow rates during the combustion tests of the CB sub-bituminous coal ($\lambda = 1.25$).

159 All the results related to the combustion tests —sections 3.2, 3.3, 3.4— have been
160 obtained from measurements taken under steady-state operation (mass flow rates,
161 temperatures, pressures and flue gases composition). Once the furnace temperature set-
162 point is achieved, coal feeding starts. After a short transient period, composition of flue
163 gases is stabilized and then operation reaches the steadiness. Data are recorded every 5
164 seconds, and steady periods can last up to 60 minutes. Flame temperature inside the
165 reactor is higher than the furnace set-points, and only one electrical furnace (the
166 bottommost one) is supplying its full power during the combustion tests.

167 Solid residues in cyclone were also collected during the steady-state regime. Ash
168 weight fractions in these solid residues were determined according to the standard UNE-
169 32-004-84. Coal burnout degree β was calculated by the ash tracer method:

$$170 \quad \beta = \frac{\alpha_f - \alpha_i}{\alpha_f(1 - \alpha_i)} \quad (2)$$

171 where α_f is the ash weight fraction (dry basis) of solid residues recovered in the cyclone
172 and α_i is the ash weight fraction (dry basis) of the fired coal.

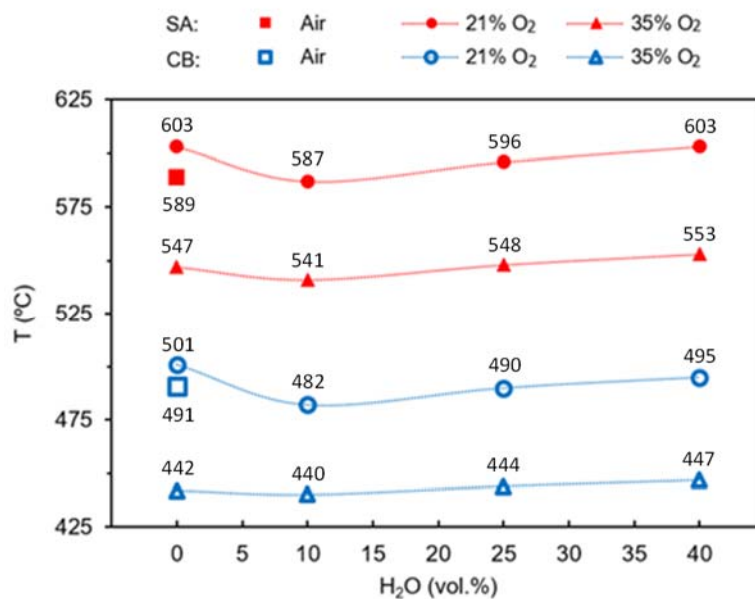
173 The closures of elemental carbon balances and heat balances have been done for the
174 combustion tests. The deviations of the mass balances range $\pm 4\%$, while the deviations of
175 the heat balances are comprised within $\pm 6\%$. The heat balances can be only closed for the
176 tests with the higher steam concentrations (25% and 40% vol.), since then the bottom

177 probe is not water-cooled –this prevents the condensing in flue gases prior to the cyclone
178 and filter, and a possible blockage–. Anyway, the low deviations in the available mass
179 and heat balances support the reliability of the results obtained.

180 3. Results and discussion.

181 3.1. Ignition.

182 Figure 2 displays the results for the ignition temperatures of both coals, under air
183 (21/79% O₂/N₂) and several O₂/CO₂ and O₂/H₂O/CO₂ conditions. The larger amount of
184 volatile matter in the CB sub-bituminous coal leads to lower values of the ignition
185 temperatures in comparison to the SA bituminous one. But the effect of changing the
186 atmosphere is quite similar for both coals.



187
188 **Figure 2.-** Ignition temperatures under air and different O₂/CO₂ and O₂/H₂O/CO₂ atmospheres (steam is
189 added as CO₂ replacement). SA: bituminous coal. CB: sub-bituminous coal.

190

191 When 79% N₂ is substituted by 79% CO₂, an increase is observed in the ignition
192 temperatures (14 K for the bituminous and 10 K for the sub-bituminous). Due to the
193 higher specific heat of CO₂ in comparison with N₂, the temperature increase of the
194 CO₂-containing atmosphere around the particle is comparatively lower during the heat
195 release produced by the initial oxidation of volatiles. Besides, O₂ diffusivity in CO₂ is also

196 lower than in N₂. If the O₂ concentration is risen, from 21/79% O₂/CO₂ to 35/65% O₂/CO₂,
197 the ignition temperature decreases (56 K for SA and 59 K for CB) due to the higher
198 oxidation rates caused the by the oxygen partial pressure [4, 6].

199 When 10% H₂O is added as CO₂ replacement in the 21% O₂ cases, there is an
200 advancement of the ignition: a decrease of 16 K for the SA bituminous coal and 19 K for
201 the CB sub-bituminous one. Several phenomena explain this reduction of the ignition
202 temperature: 1) the lower value of the molar specific heat of H₂O in comparison with
203 CO₂, 2) the higher O₂ diffusivity in H₂O in comparison to CO₂, and 3) the increase of H₂
204 concentration due both to the char gasification by steam and to the water-shift reaction
205 in the gas-phase [5, 9, 10]. This influence of the 10% H₂O addition can be also observed
206 for the 35% O₂ atmospheres, but with a more limited extent.

207 However, if the steam concentration is increased from 10% to 25% the trend is
208 reversed and the ignition temperature increases. This behaviour is related, on the one
209 hand, to the increase of radiative absorption by H₂O in comparison to CO₂. According to
210 Cai et al. [6], this effect prevails over the reduction of the specific heat for large steam
211 concentrations. On the other hand, the enhancement of char gasification by steam
212 increases CO concentration in the surroundings of the particle, displacing the oxygen,
213 and reduces the temperature due to its endothermicity. The increase of ignition
214 temperature is also observed when steam is further added up to 40%. For the 21% O₂
215 atmospheres, these increases are of 16 K for the bituminous and 13 K for the sub-
216 bituminous coal, when replacing CO₂ by H₂O from 10% to 40%.

217 The effect of the progressive CO₂ substitution by H₂O results in a “U-shape” evolution,
218 firstly decreasing the ignition temperature and later increasing it. As the steam
219 concentration grows, it can be supposed that the increase of radiative heat absorption
220 and the enhancement of char gasification contribute to a delay of the ignition in
221 comparison to the lower H₂O case, prevailing over the effect caused by a larger O₂
222 diffusivity in the atmosphere.

223 When oxygen concentration is augmented from 21% to 35%, the trend is the same but
224 the evolution is flattened with softer temperature variations. The effect of the steam is
225 attenuated under high O₂ concentrations, which is consistent with previous experiences
226 [4, 8]. In comparison to the dry O₂/CO₂ atmospheres, a 40% CO₂ replacement by H₂O
227 barely affects the ignition temperature, with maximum differences of 6 K.

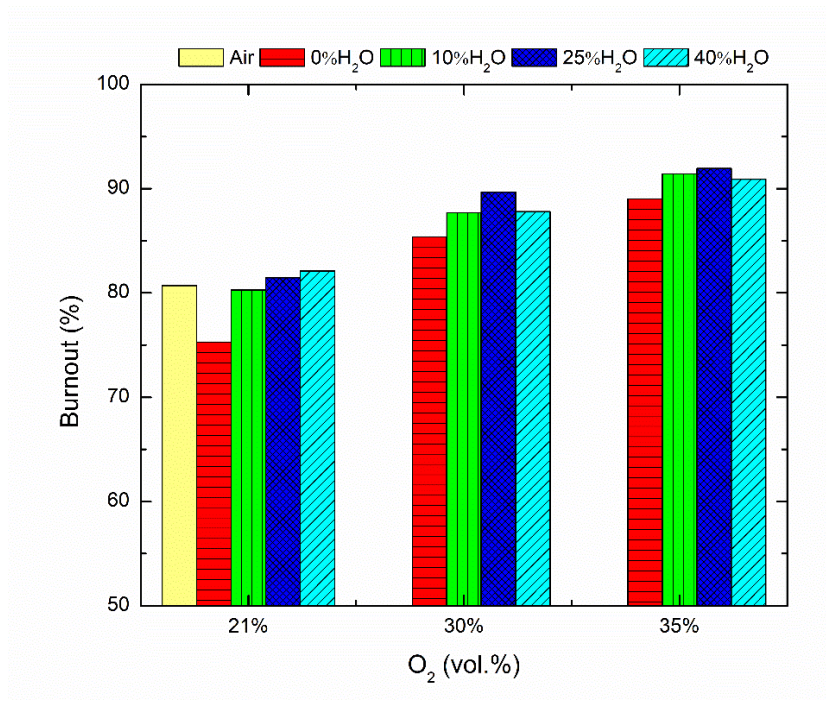
228 3.2. Burnout.

229 Figures 3 and 4 show the burnout degrees obtained under the different atmospheres
230 tested, for SA and CB coals respectively. These conversion rates have been calculated
231 according to the Eq. (2) provided in the section 2.2. Replacement of CO₂ by H₂O should
232 yield larger burnout degrees, due to the higher H₂O reactivity. This is related to the
233 increase of the gas-phase temperature, the higher O₂ diffusivity in H₂O than in CO₂, and
234 the enhancement of char gasification when H₂O concentration is augmented.

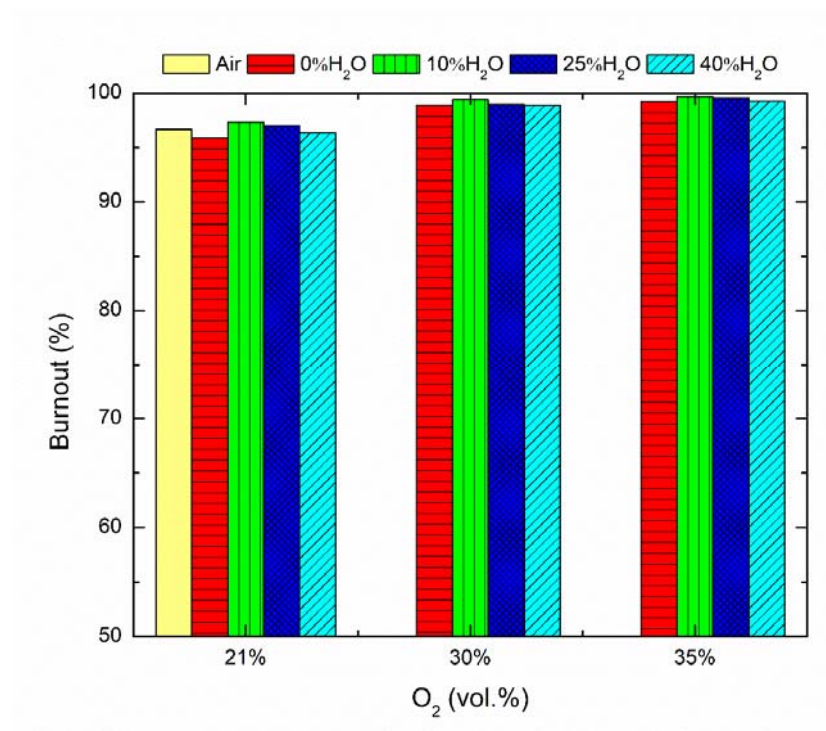
235 Since the tests were defined to keep the same residence time, burnout degrees are
236 consistently higher for the sub-bituminous coal, due to its major reactivity. Indeed, very
237 high conversion rates are obtained for all the conditions during the CB tests –see Figure
238 4–, with small differences among them. In the case of the SA bituminous coal, supply of
239 10% H₂O as CO₂ replacement always increases the burnout degree in comparison to the
240 dry O₂/CO₂ situations. For the 21% O₂ atmosphere, a significant increase of nearly 5
241 percentage points is observed. This steam-induced effect is explained by the increase of
242 both the gas-phase temperature and the O₂ diffusivity. The comparative increases also
243 observed for the 30% O₂ and 35% O₂ atmospheres are not so large; the higher conversion
244 rates and oxidant availability attenuate the rising effect caused by the 10% H₂O
245 addition. When steam is further added from 10% to 25% an additional increase of
246 burnout is obtained, but not proportionally to the steam concentration leap. These
247 differences range within 0.51–1.98 percentage points. Besides the influences on the
248 temperature and the O₂ diffusivity, H₂O also enhances char gasification in comparison to
249 CO₂ [21]. This also contributes to a larger solid-to-gas conversion rates when steam
250 concentration is augmented as CO₂ replacement.

251 Contrariwise, a different trend is shown when increasing steam addition from 25% to
252 40%. For the 21% O₂ atmosphere the variation is small, but a decrease of burnout degree
253 is detected for the 30% O₂ and 35% O₂ cases: 1.85 and 1.03 percentage points
254 respectively. The only explanation for this behaviour relies on the reduction of the char
255 specific surface caused by the enriched-H₂O atmosphere in comparison to CO₂ [22],
256 which affects the char conversion rates. To support this conclusion, BET surface areas
257 have been determined for residues samples taken from two of the bituminous coal tests:
258 35/65% O₂/CO₂ and 35/25/40% O₂/CO₂/H₂O. The used technique is N₂ isothermal
259 adsorption at 77 K, determined with a gas sorption analyzer ASAP 2020 (Micromeritics)
260 in a certified laboratory. The samples were previously degassed at 250 °C during 5 hours.

261 The BET surface areas obtained are 164.5 m²/g (35/65% O₂/CO₂) and 107.5 m²/g
 262 (35/25/40% O₂/CO₂/H₂O), which means a reduction of 34.6%.



263
 264 **Figure 3.-** Burnout degree obtained under air and different O₂/CO₂ and O₂/H₂O/CO₂ atmospheres
 265 (steam is added as CO₂ replacement), for the SA bituminous coal.



266
 267 **Figure 4.-** Burnout degree obtained under air and different O₂/CO₂ and O₂/H₂O/CO₂ atmospheres
 268 (steam is added as CO₂ replacement), for the CB sub-bituminous coal.

269 The effect of steam on the burnout degree for the CB sub-bituminous coal is partially
270 hindered by the high conversion rates achieved under all the atmospheres, as shown in
271 Figure 4. Anyway, although in a much lower extent, the trend is similar to the discussed
272 for the high-rank coal. Replacement of 10% CO₂ by H₂O yields an increase of burnout
273 degree for all the three O₂ concentrations (0.45–1.45 percentage points), the maximum
274 values are not obtained for the 40% H₂O cases, and the effect of steam on burnout is
275 attenuated when atmospheres are enriched in O₂.

276 The slight burnout decrease observed when increasing steam concentration from 10%
277 to 25% and to 40% is again explained by the decrease of the char specific surface.
278 According to Feng et al. [23], the lower the rank of the coal, the more the pore
279 development inside the char structure due to a quick precipitation of volatile matter.
280 Pallarés et al. [24] reported a maximum reduction of 43% in BET specific surfaces for a
281 high volatile fuel, when replacing CO₂ by H₂O for activation. These experiences are
282 consistent with the observations in Figures 3 and 4: the maximum burnout degree was
283 detected for the 35/10% O₂/H₂O case when firing the CB sub-bituminous coal, but it was
284 for the 35/25% O₂/H₂O case when firing the SA bituminous one. Notwithstanding, the
285 high reactivity of the sub-bituminous coal brings burnout to be very little sensitive to the
286 firing atmosphere.

287 The burnout degrees under conventional air combustion are also included in Figures 3
288 and 4: 80.7% for the SA coal and 96.7% for the CB one. The shift from O₂/N₂ to O₂/CO₂
289 combustion involves a burnout decrease, due to the reduction of the gas temperature
290 caused by the higher specific heat of CO₂ compared to N₂, and the lower diffusivity of O₂
291 in CO₂ than in N₂. As explained in the previous paragraphs, steam addition as CO₂
292 replacement produces the opposite effect, thereby resulting in similar or higher burnout
293 values than the obtained under air combustion.

294 3.3. CO in flue gases.

295 Burnout degree accounts for the solid-to-gas conversion, but it does not provide
296 information about the evolution to final products in the gas-phase. This can be indicated
297 by the presence of carbon monoxide in the flue gases leaving the reactor. CO specific
298 concentrations in flue gases are shown in Tables 6 and 7, for the SA and CB coals
299 respectively. It is clearly seen in these tables that CO levels are significantly lowered
300 when the atmosphere is O₂-enriched. Indeed, the concentrations are below the detection
301 limit for some of the experiments with the CB sub-bituminous coal.

	Air	21% O ₂	30% O ₂	35% O ₂
0% H ₂ O	5.7	7.1	3.2	2.3
25% H ₂ O	—	6.6	2.2	1.2
40% H ₂ O	—	16.0	2.8	2.1

302 **Table 6.-** CO specific emissions (mg/g_{coal}) obtained under air and different O₂/CO₂ and O₂/H₂O/CO₂
303 atmospheres (steam is added as CO₂ replacement), for the SA bituminous coal.

304

	Air	21% O ₂	30% O ₂	35% O ₂
0% H ₂ O	2.7	9.6	1.1	0.2
25% H ₂ O	—	6.0	0.2	0.0
40% H ₂ O	—	7.7	2.9	0.2

305 **Table 7.-** CO specific emissions (mg/g_{coal}) obtained under air and different O₂/CO₂ and O₂/H₂O/CO₂
306 atmospheres (steam is added as CO₂ replacement), for the CB sub-bituminous coal.

307 The CO₂ replacement by H₂O can affect to CO detected at reactor outlet by several,
308 overlapped pathways. On the one hand, steam enhances char gasification in comparison
309 to CO₂ but, on the other hand, O₂ diffusivity is higher in H₂O than in CO₂. Whilst the
310 former promotes CO release, the latter enhances CO oxidation to CO₂. Besides, steam
311 gasification effects are weakened for high O₂ concentrations, according to Hecht et al.
312 [22]. In addition, as discussed in the following section, H₂O also plays a role in the
313 NO formation/depletion mechanisms, and NO can interact with CO evolving towards
314 CO₂ and N₂.

315 The results shown in Tables 6 and 7 point to a decrease in CO concentrations when
316 CO₂ is replaced in a rate of 25% H₂O: all they are lower than the measured under the dry
317 O₂/CO₂ atmospheres. But the trend is reversed for the 40% H₂O addition, even
318 surpassing in some cases the levels corresponding to the dry atmospheres. The effect is
319 more relevant for the high-rank coal and the poorer O₂ atmosphere (21%).
320 According to these observations, large steam addition significantly enhances char
321 gasification promoting CO release, which cannot be totally compensated by the increase
322 of oxidant diffusivity along the reactor height. Anyway, all the values are very low
323 (below 3.2 mg CO/g coal) for the 30% and 35% O₂ atmospheres, independently of the coal
324 rank or the steam concentration.

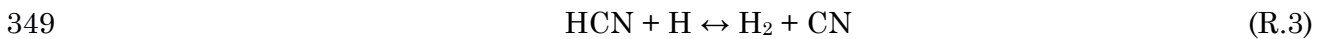
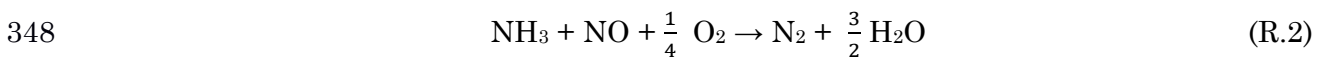
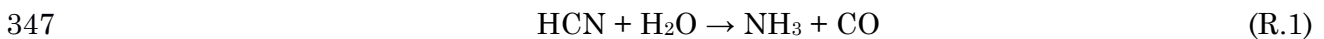
325 Aiming at relating the operating conditions with the carbon behaviour, an index has
326 been defined as the ratio of carbon solid-to-gas conversion divided by the burnout degree

327 (i.e. a comparison of the carbon conversion with the fuel averaged conversion). This index
328 has been obtained from the carbon content in the coal and the CO and CO₂
329 concentrations in flue gases. The results have been comprised in the range 0.95–0.98 for
330 the bituminous coal and 0.98–0.99 for the sub-bituminous coal. Differences are very
331 small, and cannot be related to the specifics of every test.

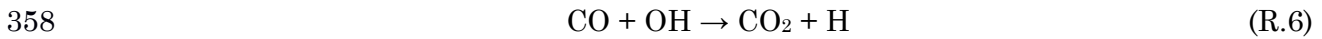
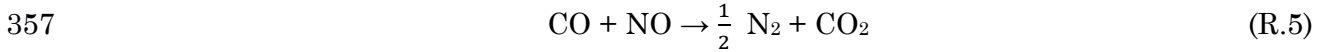
332 3.4. NO formation.

333 The extent of NO_x formation and reduction under O₂/CO₂ combustion has already
334 been experimentally characterized for a wide range of fuels and conditions [13, 25–28],
335 but large steam concentrations under oxy-steam combustion can result in very different
336 insights. Steam participates in both homogeneous reactions (involving N-volatiles) and
337 heterogeneous ones (involving N-char), then the fuel rank is also a question that must be
338 accounted.

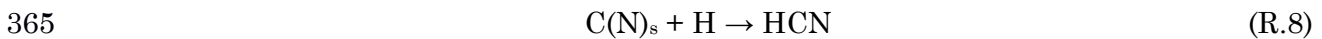
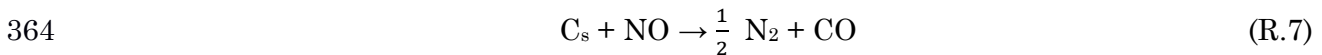
339 CO₂ replacement by H₂O leads to an increase of gas temperature and O₂ diffusivity, as
340 commented in previous sections, which increases the oxidation rates of N-fuel to NO.
341 On the contrary, steam can contribute to reduce or inhibit NO formation by different
342 ways. In the gas-phase, steam interacts with HCN over 600 °C according to the reaction
343 R.1 [16, 29, 30], competing with HCN oxidation and releasing NH₃ that can further
344 reduce NO (R.2). Besides, large steam concentration promotes the presence of an OH+H
345 radical pool in the flame, also competing with HCN oxidation through the reactions R.3
346 and R.4 [26].



351 In comparison to CO₂, steam intensifies char gasification releasing CO that can
352 contribute to reduce NO by the homogeneous reaction (R.5), catalysed by the char
353 surface [31]. This reducing effect can be attenuated by the presence of OH radicals, since
354 they contribute to CO depletion by means of the reaction (R.6). These opposite trends
355 were suggested by Zhijun et al. [18] to explain H₂O/CO₂ ratios minimizing NO formation
356 rates.



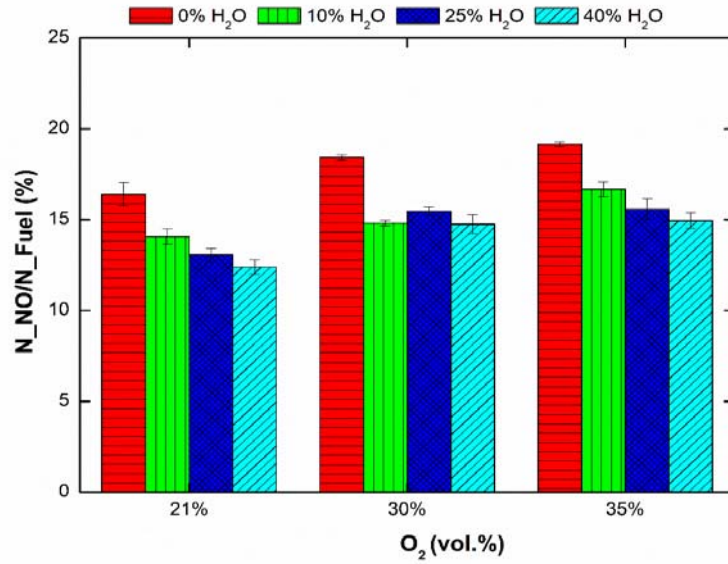
359 Enhancement of char gasification by steam increases carbon-free sites on the char
360 surface, which can reduce NO by the heterogeneous reaction R.7 [31]. Competitively,
361 char also reacts with H radicals releasing HCN according to reaction R.8 [32]. The fate of
362 HCN in the gas-phase will produce either NO by oxidation or N₂ by reduction
363 mechanisms.



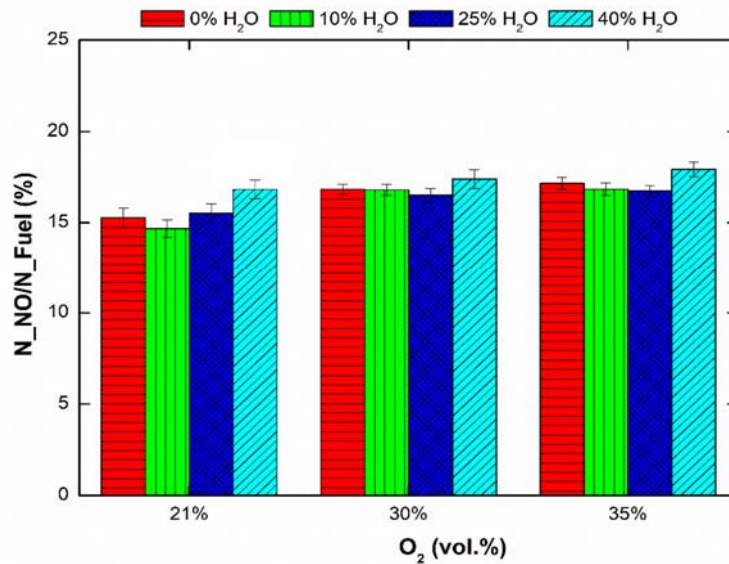
366 In order to ascertain the role of steam addition on the NO formation for the two coals
367 selected in this work, fuel-N to NO mass conversion rates were calculated for all the
368 O₂/CO₂/H₂O tests previously presented in Tables 4 and 5: three oxygen concentrations
369 (21, 30 and 35%), varying steam fraction in the range 0–40% and oxygen excess
370 $\lambda = 1.25$. The mean results and standard deviations are depicted in Figures 5 and 6, for
371 SA and CB coals respectively. The maximum standard deviations of the recorded NO
372 measurements during the steady-state operation were comprised in the range 0.5–3.5%
373 of the mean values.

374 As concerns the CB sub-bituminous coal, see Figure 6, the effect of the CO₂
375 replacement by H₂O is small if compared to the SA bituminous coal (Figure 5). For low
376 rank solid fuels, HCN release is attenuated in comparison to NH₃ one, especially under
377 wet conditions [33]. Then, the extent of the HCN–H₂O mechanisms is more limited. No
378 detailed measurements are available in the reactor to discern the role of HCN and NH₃,
379 but the lower variations of the conversions for the CB coal tests are consistent with that
380 limited extent. These limited reductions in the conversion levels are observed in Figure 6
381 when 10% H₂O is added, with a maximum decrease of 3.5% for the 21% O₂ case. This is
382 reversed in the 40% H₂O tests, even overpassing the conversion rates obtained for the
383 dry O₂/CO₂ atmospheres. Moreover, the effect of steam is smoothed as the atmosphere is
384 enriched in O₂. The trend observed in Figure 6, where an optimum H₂O value is leading
385 to the lower fuel-N to NO conversion rate, may be explained by the opposite, overlapped
386 mechanisms in the gas-phase. Initially, for low steam rates, the reductions given by the

387 set of reactions R.1 to R.4 seem to lead to a diminution in comparison to the dry cases,
 388 but for higher steam concentrations the enhancement of the oxidation rates prevails.
 389



390
 391 **Figure 5.-** Fuel-N to NO conversions obtained under different O₂/CO₂ and O₂/H₂O/CO₂ atmospheres
 392 (steam is added as CO₂ replacement), for the SA bituminous coal.



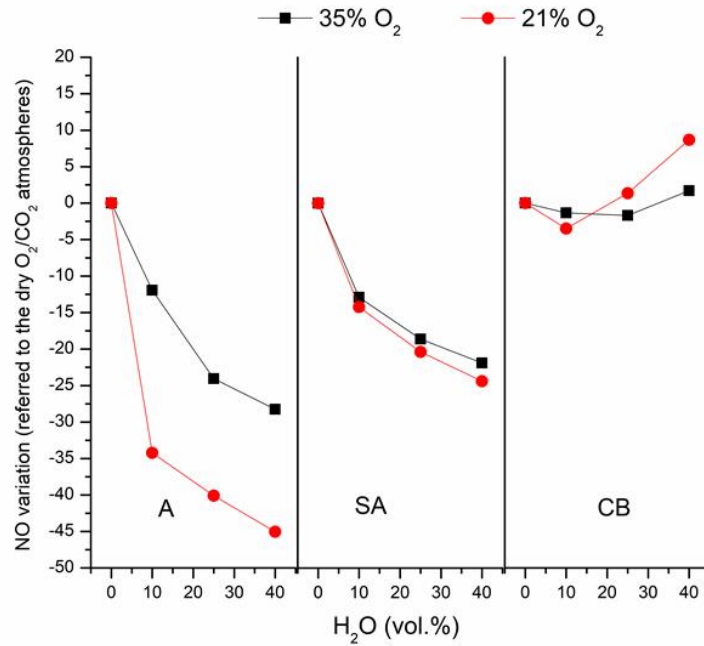
393
 394 **Figure 6.-** Fuel-N to NO conversions obtained under different O₂/CO₂ and O₂/H₂O/CO₂ atmospheres
 395 (steam is added as CO₂ replacement), for the CB sub-bituminous coal.

396 The results in Figure 5, related to the SA bituminous coal, follow a very different
397 trend to those shown in Figure 6, what points to the effect of the coal rank. Significant
398 decreases in the conversion rates to NO are obtained, for all the O₂ levels, when 10%
399 H₂O replaces CO₂. Further decrements are obtained when 40% H₂O is added to the
400 atmospheres, however not proportional to the increase of the steam percentage. This
401 behaviour is related to the composition of the SA coal, whose fixed carbon/volatiles ratio
402 is 1.9 times higher than the sub-bituminous one (in dry and ash free basis). The observed
403 reduction in the conversions to NO may be mostly related to the intensified gasification
404 caused by H₂O. Heterogeneous reaction R.7 with fixed carbon and homogeneous reaction
405 R.5 with CO (catalysed by char) are influential mechanisms. HCN–H₂O interaction also
406 contribute to the reduction, as well as other intermediate species (CN, NCO, HNCO)
407 reacting with radicals H and OH [26]. The increase in steam concentrations from 10% to
408 40%, thus rising O₂ diffusivity, does not overturn the decreasing trend for conversion to
409 NO and just attenuates it.

410 To better see the different effects observed between the fired coals, Figure 7 compares
411 the accumulative variation (%) of fuel-N to NO mass conversion rates when H₂O is
412 replacing CO₂ in the atmosphere. A third coal is also included for comparison purposes:
413 high-rank anthracite, which was tested in the same facility and under the same
414 conditions. Details about those tests and specific results can be found in reference [8]. As
415 seen in the Figure 7, the higher the coal rank, the larger the influence of steam in
416 reducing NO formation rates: maximum reductions of 45% in the case of the anthracite,
417 and 24% in the case of the SA bituminous coal. For the CB sub-bituminous coal, the
418 reduction is very limited and only detected for the lower steam concentrations, and an
419 increase of 2–9% in NO is obtained for the 40% H₂O tests.

420 High rank coals would demand an increase of oxygen excesses to complete conversion,
421 and it is well-known that this would lead to an increase on NO formation rates from the
422 nitrogen bound in the fuel. For this reason, additional tests were carried out increasing
423 oxygen excess (over stoichiometry) from $\lambda = 1.25$ to $\lambda = 1.35$ and $\lambda = 1.45$ –flow rates
424 defined to keep constant the residence time in the reactor, same as explained in section
425 2.3.2–. Figure 8 summarizes the results obtained, showing the accumulative
426 variation (%) of fuel-N to NO conversion rates as a function of the oxygen excess. The
427 extent of the increases found for anthracite and bituminous coal is, in all cases, lower
428 than the decreases respectively found for the 40% H₂O atmospheres in Figure 7.

429



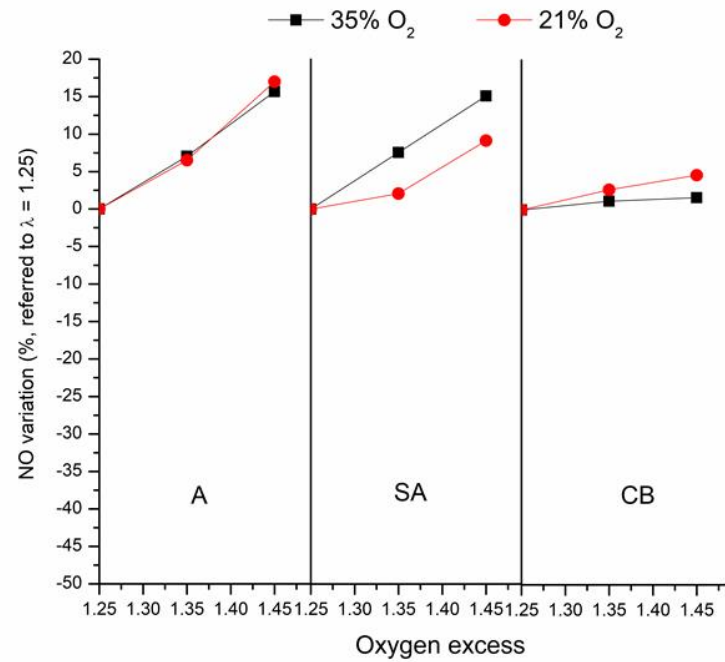
431

432

Figure 7.- Comparison of the accumulative variation (%) in fuel-N to NO mass conversion for different H₂O percentages, for anthracite (A), bituminous coal (SA) and sub-bituminous coal (CB). Anthracite results can be consulted in Ref. [8].

433

434



435

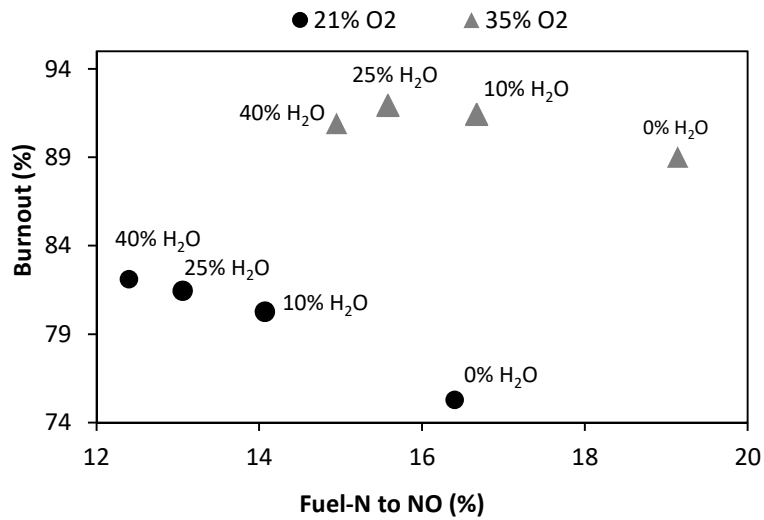
436

Figure 8.- Comparison of the accumulative variation (%) in fuel-N to NO mass conversion for different oxygen excesses, for anthracite (A), bituminous coal (SA) and sub-bituminous coal (CB). Anthracite results can be consulted in Ref. [8].

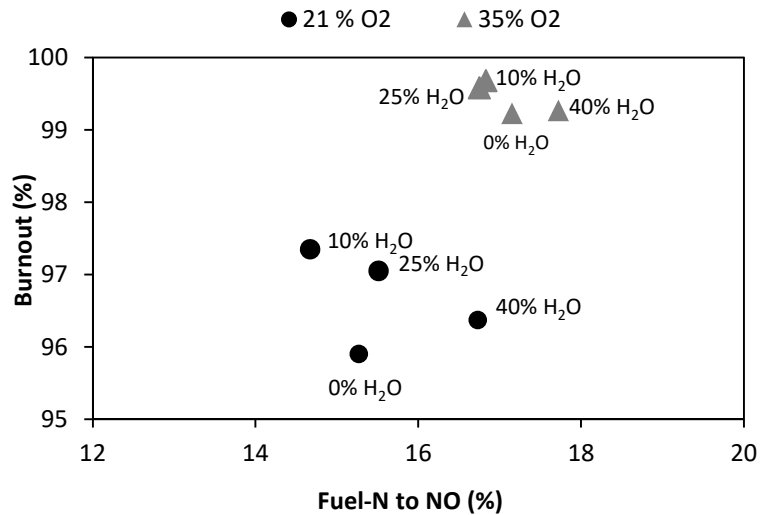
437

438

439 To conclude, it is worth mentioning that CO₂ replacement by H₂O is leading to a
 440 twofold benefit for the SA bituminous coal, in comparison to the dry situations: an
 441 increase of burnout degrees along with a decrease of fuel-N to NO mass conversion rates,
 442 for every O₂ concentration. This joint outcome is represented in Figure 9, merging the
 443 results previously shown in Figures 3 and 5. A similar representation is given in Figure
 444 10 for the CB sub-bituminous coal: in this case, the CO₂ replacement by H₂O increases
 445 the NO formation rates for the 40% H₂O atmospheres in comparison to the dry ones.



446
 447 **Figure 9.-** Fuel-N to NO conversions vs. burnout degrees, for the SA bituminous coal.
 448



449
 450 **Figure 10.-** Fuel-N to NO conversions vs. burnout degrees, for the CB sub-bituminous coal.

451 **Conclusions**

452 The combustion characteristics of two different coals have been experimentally
453 determined in an entrained flow reactor, for a set of O₂/N₂, O₂/CO₂ and O₂/H₂O/CO₂
454 atmospheres. Besides the influence of the coal rank, the effect of replacing CO₂ by H₂O
455 on the ignition, burnout and NO formation has been sought. Steam concentration was
456 increased up to 40%, while oxygen concentration up to 35%. The following outcomes have
457 been obtained:

- 458
459 • Regardless the coal type and O₂ concentration, it is observed that: 1) addition
460 of steam in low rates (10%) decreases ignition temperature, 2) the trend is
461 reversed when steam concentration is further incremented to 25% and 40%.
462 The differences in ignition temperatures are minimally higher for the sub-
463 bituminous coal. Replacement of 40% CO₂ by H₂O yields a small variation of
464 the ignition temperature in comparison to the dry atmospheres.
- 465
466 • The burnout degree of the bituminous coal is increased when CO₂ is replaced
467 by H₂O in the firing atmosphere, but the largest conversions are not detected
468 for the maximum steam concentrations. The extent of the steam influence on
469 the burnout degree is attenuated when the atmosphere is enriched in O₂. As
470 concerns the sub-bituminous coal, its reactivity produces very high conversion
471 rates for all the atmospheres tested and the effect of CO₂ replacement by H₂O
472 is similar but much more narrowed.
- 473
474 • The influence of steam on NO formation is very different depending on the coal
475 rank. A significant decrease in fuel-N to NO conversion rate is observed for the
476 bituminous coal when replacing 40% CO₂, but an increase is observed for the
477 sub-bituminous one. Their different volatiles/char ratio determines the extent
478 of homogeneous and heterogeneous mechanisms in which steam is involved.
479 The effect of oxygen excess on NO formation has been proved to be less
480 influential than the effect of the steam concentration.

481

482 **Acknowledgements**

483 The work described in this paper has been funded by the R+D Spanish National
484 Program from the Spanish Ministry of Science, Innovation and Universities, under the
485 Projects ENE2015-67448 and RTI2018-094488, and the Grant BES-2016-078573.

486 Dr. M.C. Mayoral, Dr. J.M. Andrés and Dr. J. Pallarés are gratefully acknowledged
487 for providing the samples of the coals. The Service of Electronic Instrumentation
488 (University of Zaragoza) is also acknowledged for their support in the development of the
489 SCADA at the experimental facility.

490

491 **References**

- 492 [1] International Energy Agency, <https://www.iea.org/fuels-and-technologies/coal>, 2020
493 [14/05/2020].
- 494 [2] C. Salvador, Modeling, design and pilot-scale experiments of CANMET's advanced
495 oxy-fuel/steam burner, 2nd Workshop International Oxy-Combustion Research
496 Network, Windsor, CT, USA, 2007.
- 497 [3] S. Seepana, S. Jayanti, Steam-moderated oxy-fuel combustion, *Energy Convers*
498 *Management* 51 (2010) 1981–1988.
- 499 [4] W. Prationo, L. Zhang, Influence of steam on ignition of Victorian brown coal
500 particle stream in oxy-fuel combustion: In-situ diagnosis and transient ignition
501 modelling, *Fuel* 181 (2016) 1203–1213.
- 502 [5] R.B. Kops, F.M. Pereira, M. Rabaçal, M. Costa, Effect of steam on the single
503 particle ignition of solid fuels in a drop tube furnace under air and simulated oxy-
504 fuel conditions, *Proceedings of the Combustion Institute* 37 (2019) 2977–2985.
- 505 [6] J. Riaza, L. Álvarez, M.V. Gil., C. Pevida, J.J. Pis, F. Rubiera. Effect of oxy-fuel
506 combustion with steam addition on coal ignition and burnout in an entrained flow
507 reactor, *Energy* 36 (2011) 5314–5319.
- 508 [7] L. Cai, C. Zou, Y. Guan, H. Jia, L. Zhang, C. Zheng, Effect of steam on ignition of
509 pulverized coal particles in oxy-fuel combustion in a drop tube furnace, *Fuel* 182
510 (2016) 958–966.
- 511 [8] A.I. Escudero, M. Aznar, L. I. Díez, M. C. Mayoral, J. M. Andrés, From O₂/CO₂ to
512 O₂/H₂O combustion: The effect of large steam addition on anthracite ignition,
513 burnout and NO_x formation, *Fuel Processing Technology* 206 (2020) 106432.
- 514 [9] C. Zou, L. Cai, D. Wu, Y. Liu, S. Liu, C. Zheng, Ignition behaviors of pulverized coal
515 particles in O₂/N₂ and O₂/H₂O mixtures in a drop tube furnace using flame
516 monitoring techniques, *Proceedings of Combustion Institute* 35 (2015) 3629–3636.
- 517 [10] Z. Hao, Y. Li, N. Li, K. Cen, Experimental investigation of ignition and combustion
518 characteristics of single coal and biomass particles in O₂/N₂ and O₂/H₂O, *Journal of*
519 *the Energy Institute* 92 (2019) 502–511.

- 520 [11] L. Álvarez, M. Gharebaghi, M. Pourkashanian, A. Williams, J. Riazza, C. Pevida,
521 J.J. Pis, F. Rubiera, CFD modelling of oxy-coal combustion in an entrained flow
522 reactor, *Fuel Processing Technology* 92 (2011) 1489–1497.
- 523 [12] X. Jiang, X. Huang, J. Liu, X. Han, NO_x emission of fine and superfine pulverized
524 coal combustion in O₂/CO₂ atmosphere, *Energy and Fuels* 24 (2010) 6307–6313.
- 525 [13] H. Hashemi, S. Hansen, M.B. Toftegaard, K.H. Pedersen, A.D. Jensen, K. Dam-
526 Johansen, et al., A model for nitrogen chemistry in oxy-fuel combustion of
527 pulverized coal, *Energy and Fuels* 25 (2011) 4280–4289.
- 528 [14] H. Liu, R. Zailani, B.M. Gibbs, Comparisons of pulverized coal combustion in air
529 and in mixtures of O₂/CO₂, *Fuel* 84 (2005) 833–840.
- 530 [15] W. Moron, W. Rybak, NO_x and SO₂ emissions of coals, biomass and their blends
531 under different oxy-fuel atmospheres, *Atmospheric Environment* 116 (2015) 65–71.
- 532 [16] L. Álvarez, J. Riazza, M.V. Gil, C. Pevida, J.J. Pis, F. Rubiera, NO emissions in oxy-
533 coal combustion with the addition of steam in an entrained flow reactor,
534 *Greenhouse Gases Science Technology* 1 (2011) 180–190.
- 535 [17] L. Yupeng, S. Rui, W. Jiangquan, W. Zhuozhi, W. Min, Song Zhenyu, Effect of H₂O
536 on char-nitrogen conversion during char-O₂/H₂O combustion under high-
537 temperature entrained flow conditions, *Combustion and Flame* 207 (2019) 391–
538 405.
- 539 [18] S. Zhijun, S. Su, J. Xu, K. Xu, S. Hu, Y. Wang, L. Jiang, N. Si, Y. Zhou, S. S. A.
540 Syed-Hassan, A. Zhang, J. Xiang, Effects of H₂O on NO emission during oxy-coal
541 combustion with wet recycle, *Energy and Fuels* 31 (2017) 8392–8399.
- 542 [19] J. Faúndez, B. Arias, F. Rubiera, A. Arenillas, X. García, A.L. Gordon, J.J. Pis,
543 Ignition characteristics of coal blends in an entrained flow furnace, *Fuel* 86 (2007)
544 2076–2080.
- 545 [20] J. Riazza, J. Gibbins, H. Chalmers, Ignition and combustion of single particles of
546 coal and biomass, *Fuel* 202 (2017) 650–655.
- 547 [21] E. S. Hecht, C. R. Shaddix, M. Geier, A. Molina, B. S. Haynes, Effect of CO₂ and
548 steam gasification reactions on the oxy-combustion of pulverized coal char,
549 *Combustion and Flame* 159 (2012) 3437–3447.
- 550 [22] J. Xu, S. Su, Z. Sun, N. Si, M. Qing, L. Liu, S. Hu, Y. Wang, J. Xiang, Effects of
551 H₂O gasification reaction on the characteristics of chars under oxy-fuel combustion
552 conditions with wet recycle, *Energy and Fuels* 30 (2016) 9071–9079.
- 553 [23] D. Feng, D. Guo, Y. Zhao, H. Tan, G. Chang, T. Zhang, S. Sun, Formation and
554 O₂/CO₂ combustion characteristics of real-environment coal char in high-
555 temperature oxy-fuel conditions, *Journal of the Energy Institute* 92 (2019) 1670–
556 1682.

- 557 [24] J. Pallarés, A. González-Cencerrado, I. Arauzo, Production and characterization of
558 activated carbon from barley straw by physical activation with carbon dioxide and
559 steam, *Biomass and Bioenergy* 115 (2018) 64–73.
- 560 [25] P. Glarborg, A.D. Jensen, J.E. Johnsson, Fuel nitrogen conversion in solid fuel fired
561 systems, *Progress in Energy and Combustion Science* 29 (2003) 89–113.
- 562 [26] P. Glarborg, J. A. Miller, B. Ruscic, S. J. Klippenstein, Modeling nitrogen
563 chemistry in combustion, *Progress in Energy and Combustion Science* 67 (2018)
564 31–68.
- 565 [27] L. Chen, S. Z. Yong, A. F. Ghoniem, Oxy-fuel combustion of pulverized coal:
566 Characterization, fundamentals, stabilization and CFD modelling, *Progress in*
567 *Energy and Combustion Science* 38 (2012) 156–214.
- 568 [28] T. Aihara, K. Matsuoka, T. Kyotani, A. Tomita, Mechanism of N₂ formation during
569 coal char oxidation, *Proceedings of the Combustion Institute* 28 (2000) 2189–2195.
- 570 [29] S. Schafer, B. Bonn, Hydrolysis of HCN as an important step in nitrogen oxide
571 formation in fluidised combustion, Part 1: homogeneous reactions, *Fuel* 79 (2000)
572 1239–1246.
- 573 [30] C. Ndibe, R. Spörl, J. Maier, G. Scheffknecht, Experimental study of NO and NO₂
574 formation in a PF oxy-fuel firing system, *Fuel* 107 (2013) 749–756.
- 575 [31] I. Aarna., E.M. Suuberg, A review of the kinetics of the nitric oxide-carbon reaction,
576 *Fuel* 76 (1997) 475–491.
- 577 [32] A. Arenillas, F. Rubiera, J.J. Pis, Nitric oxide reduction in coal combustion: Role of
578 char surface complexes in heterogeneous reactions, *Environmental Science &*
579 *Technology* 36 (2020) 5498–5503.
- 580 [33] F-J. Tian, H. Wu, J. Yu, L. J. McKenzie, S. Konstantinidis, J. Hayashi, T. Chiba,
581 C-Z. Li, Formation of NO_x precursors during the pyrolysis of coal and biomass, Part
582 VIII: effects of pressure on the formation of NH₃ and HCN during the pyrolysis and
583 gasification of Victorian brown coal in steam, *Fuel* 84 (2005) 2102–2108.